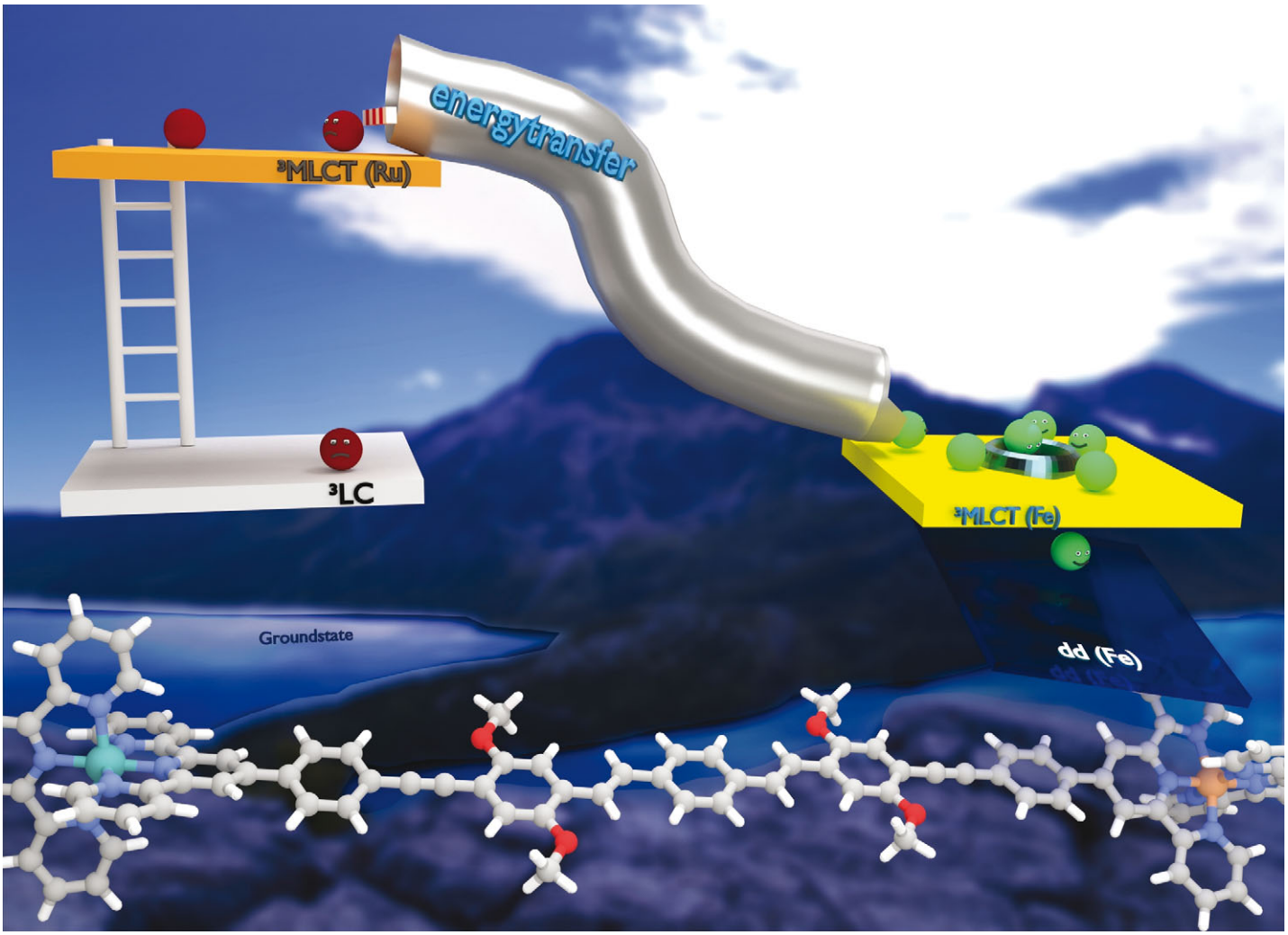


**Showcasing research from the laboratory of Prof. Dr Benjamin Dietzek at the Leibniz Institute of Photonic Technology, Jena, Germany.**

Title: Energy transfer and formation of long-lived $^3$MLCT states in multimetallic complexes with extended highly conjugated bis-terpyridyl ligands

Heterometallic complexes in which metal centers are connected by functional bridging chromophores are components for light-harvesting antenna units in potential artificial photosynthetic model systems. The present work includes a trinuclear Ru(II)–Fe(II)–Ru(II) complex with extended and highly conjugated 2,2′:6′,2″-terpyridine ligands. The compound shows after photoexcitation of the Ru-based $^1$MLCT band efficient, yet incomplete, energy transfer from the Ru- towards the Fe-based-$^3$MLCT state. This state is remarkably long-lived (23 ps) in view of the very fast spin-crossover (≪1 ps) typically observed in Fe(II)-polypyridine complexes.

## As featured in:


See Benjamin Dietzek *et al.*, *Phys. Chem. Chem. Phys.*, 2016, **18**, 2350.

ROYAL SOCIETY OF CHEMISTRY

www.rsc.org/pccp

Registered charity number: 207890

PCCP

PAPER

View Article Online
View Journal | View Issue



Cite this: *Phys. Chem. Chem. Phys.*, 2016, **18**, 2350

# Energy transfer and formation of long-lived $^3$MLCT states in multimetallic complexes with extended highly conjugated bis-terpyridyl ligands†

Maria Wächtler,[a] Joachim Kübel,[ab] Kevin Barthelmes,[cd] Andreas Winter,[cd] Alexander Schmiedel,[e] Torbjörn Pascher,[f] Christoph Lambert,[e] Ulrich S. Schubert[cd] and Benjamin Dietzek*[abd]

Received 28th July 2015,
Accepted 11th September 2015

DOI: 10.1039/c5cp04447b

www.rsc.org/pccp

Multimetallic complexes with extended and highly conjugated bis-2,2′:6′,2″-terpyridyl bridging ligands, which present building blocks for coordination polymers, are investigated with respect to their ability to act as light-harvesting antennae. The investigated species combine Ru(II)- with Os(II)- and Fe(II)-terpyridyl chromophores, the latter acting as energy sinks. Due to the extended conjugated system the ligands are able to prolong the lifetime of the $^3$MLCT states compared to unsubstituted terpyridyl species by delocalization and energetic stabilization of the $^3$MLCT states. This concept is applied for the first time to Fe(II) terpyridyl species and results in an exceptionally long lifetime of 23 ps for the Fe(II) $^3$MLCT state. While partial energy (>80%) transfer is observed between the Ru(II) and Fe(II) centers with a time-constant of 15 ps, excitation energy is transferred completely from the Ru(II) to the Os(II) center within the first 200 fs after excitation.

## Introduction

The design of artificial antennae systems for efficient collection of solar radiation, *i.e.*, multicomponent systems in which several molecular components absorb the incident light and channel the energy to an acceptor unit, is an active field of research.[1–8] The ultimate goal is to build systems, which are capable of harvesting light over a large part of the visible spectrum. In this respect a number of systems containing transition metal complexes have been prepared and studied.[1,2,5,9–16] Multimetallic complexes containing several metal centers connected *via* large conjugated ligands can show photoinduced energy and/or electron transfer processes between the individual chromophoric centers.[13,16,17] A challenge in the design of such systems is to control the direction of the energy/electron transfer, to transport the excitation over large distances, *e.g.*, in wirelike structures.[17–20] This can be achieved by structural and electronic variations of the bridging ligands and/or by changing metal centers and their coordination environment to create a gradient for energy or electron transport in the system.[13] In this respect, hierarchically structured coordination polymers are interesting systems for the design of artificial light-harvesting antennas. Especially, low-spin d$^6$ polypyridyl transition metal complexes play an important role in this field due to their strong absorption of light in the visible spectral range and the favorable and tunable photophysical properties of their charge-transfer states.[13,17,21–23]

In this contribution bi- and trimetallic systems are investigated, which may serve as building blocks for coordination polymers. For this purpose a bis-2,2′:6′,2″-terpyridyl ligand **L** bearing a conjugated spacer, which is closely related to the widely used poly[phenylene–vinylene] and poly[phenylene–ethynylene] conjugated polymers (Fig. 1), is used.[24,25] The strong conjugation of the bridging ligand together with the tridentate coordination site enables to build linear, rodlike structures and no stereoisomer mixtures are formed upon complexation, as it is the case for bidentate ligands.[13,17,20,26,27] The herein investigated species combine Ru(II) and Fe(II) (**RuFeRu**) or Ru(II) and Os(II) (**RuOs**) centers, which are coordinated by the terpyridyl units. This combination of metal centers in the supramolecular assembly is advantageous due to their complementary absorption features: both Fe(II) and Os(II) complexes absorb at wavelengths longer than the $^1$MLCT (metal-to-ligand charge transfer) absorption band of Ru(II)-terpyridyl centers: Fe(II) terpyridyl complexes possess a

[a] *Leibniz Institute of Photonic Technology e.V., Albert-Einstein-Straße 9, 07745 Jena, Germany. E-mail: benjamin.dietzek@ipht-jena.de; Fax: +49 (0)3641 206-390; Tel: +49 (0)3641 206-332*
[b] *Institute of Physical Chemistry and Abbe Center of Photonics, Friedrich Schiller University Jena, Helmholtzweg 4, 07743 Jena, Germany*
[c] *Laboratory of Organic and Macromolecular Chemistry (IOMC), Friedrich Schiller University Jena, Humboldtstraße 10, 07743 Jena, Germany*
[d] *Jena Center for Soft Matter (JCSM), Friedrich Schiller University Jena, Philosophenweg 7, 07743 Jena, Germany*
[e] *Institut für Organische Chemie, Universität Würzburg, Wilhelm Conrad Röntgen Research Center for Complex Material Systems, Center for Nanosystems Chemistry, Am Hubland, 97074 Würzburg, Germany*
[f] *Pascher Instruments AB, Stora Råbybyavägen 24, 22478 Lund, Sweden*
† Electronic supplementary information (ESI) available. See DOI: 10.1039/c5cp04447b

 

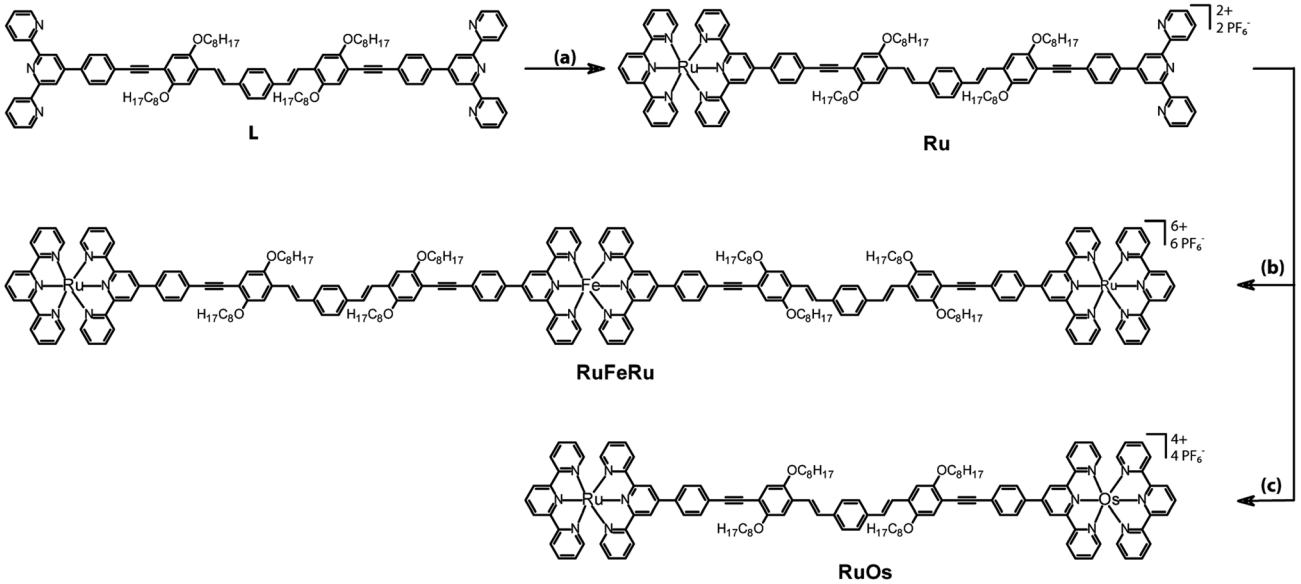


Fig. 1 Structures and synthesis of the investigated polynuclear complexes **RuFeRu** and **RuOs** and the mononuclear reference complex **Ru**. Legend: (a) $[Ru(tpy)(acetonitrile)_3](PF_6)_2$, DMF, 160 °C, 3 h; (b) $FeSO_4{\cdot}7H_2O$, dichloromethane/methanol, room temperature, 2 h; (c) (i) $Os(tpy)Cl_3$, $AgBF_4$, acetone, 70 °C, 2 h, (ii) DMA/ethylene glycol, 160 °C, 24 h.

$^1$MLCT transition at *ca.* 560 nm[28–30] and the Os(II) terpyridyl chromophore shows, besides a $^1$MLCT absorption band in the same wavelengths range as the Ru(II) $^1$MLCT transitions, a $^3$MLCT absorption band spanning the entire visible range of the absorption spectrum[17] extending the overall absorption spectrum of the assembly far into the red up to 700 nm. In these assemblies the Ru(II) centers are expected to serve as excitation energy donor while Os(II) and Fe(II) centers possess lower lying excited states and serve as potential energy accepting units.[13,15,17,18,28,31–33]

A critical property for future applicability of such structures is the excited state lifetime of the acceptor centers, which can be a crucial efficiency determining factor for subsequent reaction steps, *e.g.*, charge separation and generation of redox-equivalents. The $^3$MLCT states of Os(II)-bis(terpyridyl) chromophores possess sufficiently long lifetimes in the range of 200 ns in aerated solution at room temperature.[17] Due to the high ligand-field strength in Os complexes the energy gap between $^3$MLCT states and metal-centered (MC) ligand field states, which offer an efficient route for radiationless deactivation, is large.[17,28] This prevents deactivation of the $^3$MLCT state *via* thermal population of the MC states.[34] In the order Os(II), Ru(II) and Fe(II) the ligand field strength decreases and, hence, the MC states are significantly closer in energy to the $^3$MLCT states in comparable Ru(II) and Fe(II) complexes. Furthermore, in tridentate terpyridyl complexes additional weakening of the ligand field is observed due to the unfortunate bite angle of the terpyridyl ligand, which causes a distortion of the octahedral coordination sphere.[13,17] This further decreases the energetic separation between MC and MLCT states which is reflected in the short room-temperature lifetime of the $^3$MLCT excitation in Ru(II)-terpyridyl complexes ($[Ru(tpy)_2]^{2+}$ $\tau$ = 124 ps)[17,35] and Fe(II)-polypyridyl complexes in general ($[Fe(tpy)_2]^{2+}$, $[Fe(bpy)_3]^{2+}$ $\tau \leq 0.2$ ps).[36–43] This is also the reason why – in contrast to Ru(II) and Os(II)-polypyridyl centers – Fe(II)-polypyridiyl complexes are not established in light-harvesting applications yet, despite its high abundance and low cost of production. Only ultrafast charge separation processes on the sub 100 fs timescale are able to compete with the ultrafast deactivation to the high spin quintet state (which is probably mediated by ligand field triplet states) in Fe(II)-polypyridyl complexes,[36–42] *e.g.*, ultrafast injection of electrons into $TiO_2$.[37,44,45] Hence, to boost the applicability of Fe(II)-polypyridyl dyes in light-harvesting applications one important goal is to prolong the $^3$MLCT lifetime.

One approach to prolong the lifetime of $^3$MLCT states is to increase the relative energy of the MC states *via* coordination of ligands with high ligand field strength, *e.g.*, strong σ-donor ligands. Attractive candidates in this respect are cyclometallated ligands. In a first attempt $^3$MLCT lifetimes in Ru(II) complexes were extended by four orders of magnitude[46–48] and in Fe(II) cyclometallated complexes $^3$MLCT lifetimes of 9 ps and even 13 ps were achieved, which corresponds to an extension of the $^3$MLCT lifetime by two orders of magnitude.[49–51] A second possibility to increase the energy gap between $^3$MLCT and MC states is to coordinate stronger π-acceptor ligands, which also increases the ligand field strength, hence raises the energy of the MC states and further results in lower energies of the $^3$MLCT state. This can be achieved by substitution in the 4′-position of the terpyridyl ligand and extending the conjugated system of the terpyridyl coordination sphere. Applying this approach the lifetimes in Ru(II) complexes were extended to reach tens of ns.[27] An additional prolongation of the lifetime of the $^3$MLCT state can be achieved by applying highly extended conjugated 4′-terpyridyl ligands. In such systems low lying $^3$LC (ligand-centered) states may form equilibria with the $^3$MLCT state.[27,30,52,53] Though structures fulfilling these preconditions are known in literature,[54–56] the Fe(II) $^3$MLCT lifetimes in such systems have not been addressed yet.

A third approach was applied by Heinze *et al.*[57] by coordinating ligands with larger bite angle than the classical terpyridyl units, which increases the relative energy of MC states due to less distortion of the coordination polyhedron resulting in a stronger ligand field.[58–62] Additionally, ligands with strong electron withdrawing/electron donating character have been combined resulting in push–pull systems with low lying $^3$MLCT states.[63–65] The first attempts following this approach for Fe(II) complexes, however, did not lead to formation of a long-lived CT (charge-transfer) states.[57]

In the here investigated systems the highly conjugated bis-2,2′:6′,2″-terpyridine ligands offer the possibility to stabilize the $^3$MLCT states and additionally to form equilibria with low lying $^3$LC states as was previously reported for Ru(II) coordinated by related ligands.[66] In the following the photoinduced processes in the multimetallic systems, especially with respect to possible energy transfer pathways between the specific metal centers, will be investigated by time-resolved spectroscopy. Special emphasis will be on the $^3$MLCT lifetime of the Fe(II) $^3$MLCT states in these systems.

## Experimental section

For spectroscopic measurements all compounds were dissolved in aerated acetonitrile (spectrophotometric grade). Absorption spectra were recorded with a Lambda 750 (PerkinElmer) UV/VIS spectrometer in a cell with 1 cm pathlength. Emission spectra were recorded with a Jasco FP-6200 spectrofluorometer. For all time-resolved measurements the stability of the samples was verified by recording the absorption spectra before and after each measurement.

For the ns time-resolved transient absorption (TA) measurements the samples were excited by 5 ns pulses at 520 nm with a repetition rate of 10 Hz. The probe light is delivered by a pulsed 75 W Xe arc lamp and detected on a PMT after passing a monochromator. By switching off the probe light emission decay can be detected with ns-temporal resolution with the same set-up.

The fs time-resolved transient absorption measurements were performed in a cuvette with 1 mm path length. **Ru** and **RuFeRu** were excited by 140 fs pulses at 520 nm and 520/575 nm, respectively. A white light continuum generated in a $CaF_2$ crystal was used to probe the sample between 350 and 800 nm. The relative temporal delay between the pump and probe pulses was varied over a maximum range of 8 ns. The fs time-resolved measurements for **RuOs** were performed applying pump pulses centered at 520 and 670 nm with a duration of ~80 fs and probed by a white-light continuum between 450 and 700 nm, which is produced in a sapphire crystal. The pump pulses are delayed with respect to the probe pulses by means of an optical delay stage over a maximum range of 2 ns. The mutual polarization of the pump and probe pulses was set to magic angle.

Prior to data analysis the experimental data from the fs time-resolved measurements were chirp corrected. To avoid prominent contributions from the coherent artifact the pulse overlap region (±200 fs) around time zero was excluded in the data fitting procedure. The data were fitted with a global fitting routine applying a sum of exponential functions for data analysis. Additionally, the data for **RuFeRu** upon excitation at 520 nm were numerically fitted with a home-written algorithm for non-sequential (*e.g.*, including branching of the relaxation pathway) kinetic schemes.

For a more detailed description of the synthetic procedures, characterization, experimental set-ups and the fitting procedure the reader is referred to the ESI.†

## Results and discussion

### Synthesis

The synthesis of the bridging ligand **L**, which is used in this study, was reported recently.[67] In order to obtain heterometallic oligonuclear complexes, a two-step assembly approach had to be followed (Fig. 1). The first step was the preparation of the mononuclear Ru(II) bisterpyridyl complex **Ru** by reaction of $[Ru(tpy)(acetonitrile)_3](PF_6)_2$[68] with ligand **L** in DMF (tpy – 2,2′:6′,2″-terpyridine).[69] The trinuclear complex **RuFeRu** was prepared by addition of a methanolic Fe(II) sulphate solution to a solution of **Ru** in dichloromethane. The dinuclear complex **RuOs** was prepared by the reactions of **Ru** with silver-activated $Os(tpy)Cl_3$ in a DMAc/ethylene glycol mixture.[70]

### Steady-state absorption and emission spectroscopy

The absorption spectra of **Ru**, **RuFeRu** and **RuOs** in acetonitrile are displayed in Fig. 2. The spectra show multiple electronic transitions in the visible and UV spectral region. ππ* transitions, which are located at the terpyridine sphere, dominate at wavelengths shorter than 350 nm. At longer wavelengths the spectra contain a superposition of ligand-centered ππ* transitions and transitions which appear upon coordination of the metal center and, according to literature, most likely are due to MLCT

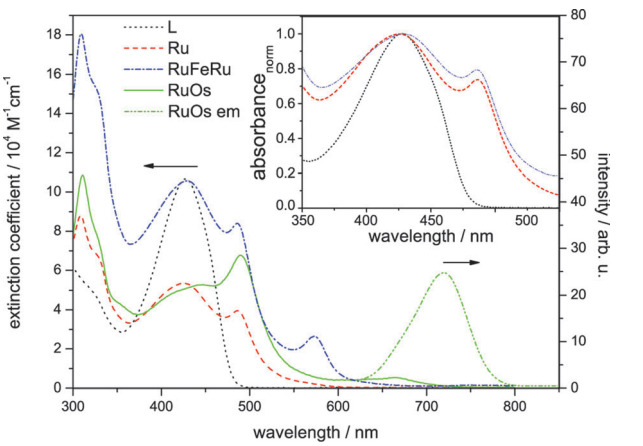


Fig. 2 Steady-state absorption spectra of **Ru**, **RuFeRu** and **RuOs** and emission spectrum of **RuOs** after excitation at 488 nm in aerated acetonitrile. For comparison the absorption spectrum of the bridging ligand **L** in dichloromethane is given. The inset shows the normalized absorption spectra of **L**, **Ru** and **RuFeRu** for comparison of the position of the LC absorption band.

transitions.[17,28–30,71] The ligand-centered ππ* transitions of the extended bridging ligand can be identified by the comparison with the absorption spectrum of the pure ligand **L** (absorption maximum at 429 nm). No significant shifts are observed in the ππ* transition upon coordination of one or two metal centers: for **Ru** the maximum of the ππ* transition is at 426 nm and for **RuFeRu** at 429 nm. For **RuOs** no separate maximum of the ππ* transition can be distinguished. The Ru(II) $^1$MLCT transitions in **Ru** and **RuFeRu** peak at 486 nm while in **RuOs** the maximum of the superimposed $^1$MLCT transitions of both the Ru(II) and Os(II) centers is at 490 nm. The $^1$MLCT transitions at the Ru(II) and Os(II) center present a mixture of transitions to the terminal tpy ligand and the 4′-substituted bridging ligand with the extended chromophore. The torsional angle between the tpy unit and the adjacent phenyl ring, which is typically in the range of 30°,[72–74] reduces conjugation but does not inhibit it completely. Hence, the chromophore is delocalized over the tpy and the directly connected phenyl ring, but – on the other hand – does not extent over the ethynyl bond.[72] When comparing the absorption spectrum of **RuFeRu** to the one of **Ru** an additional band at 574 nm is observed, which is assigned to the Fe(II) $^1$MLCT transition to the bridging ligand. Also the spectrum of **RuOs** is significantly broadened due to additional weak spin-forbidden $^3$MLCT transitions spanning the visible spectral region up to 700 nm with a maximum at 665 nm.

Only for **RuOs** a weak triplet emission could be detected at room temperature in aerated solution. This emission peaks at 720 nm and is due to $^3$MLCT phosphorescence from the Os(II) center. In all three investigated species, even the mononuclear complex **Ru**, phosphorescence from the Ru(II) $^3$MLCT state is not detectable, hence no conclusions about energy transfer between the metal centers can be drawn from emission experiments. The missing emission could be an indication for a strong delocalization of the $^3$MLCT state over the extended bridge in these systems, decreasing the oscillator strength for the radiative return to the ground state and open the competition with more prone non-radiative deactivation processes. Besides its probably low quantum yield, unambiguous detection of the Ru(II) $^3$MLCT emission in **Ru** unfortunately is additionally hampered by residual fluorescence originating from LC states in the same spectral region where the emission of the $^3$MLCT is expected (for further details see ESI,† Fig. S1 and S2). Such LC emission was reported earlier for related 2,2′:6′:2″-terpyridine complexes coordinating two highly conjugated 4′-(4-{[2,5-bis(octyloxy)-4-styrylphenyl]ethynyl}-phenyl)-2,2′:6′,2″-terpyridine ligands.[30,75] Emission originating from the Fe(II) $^3$MLCT in **RuFeRu** is not expected due to the generally observed fast deactivation of the $^3$MLCT states in Fe(II)-polypyridyl complexes either populating a non-luminescent high-spin quintet state[36–43] or rapidly repopulating the ground state *via* $^3$MC states.[50,51]

### Lifetime of long-lived excited states

The lifetime of the Os(II) $^3$MLCT based phosphorescence of **RuOs** in aerated acetonitrile at room temperature was determined to 100 ns, which is in good agreement with the decay time of the excited-state absorption (ESA) signal in ns time-resolved transient absorption (TA) measurements ($\tau$ = 84 ns) (Fig. 3).

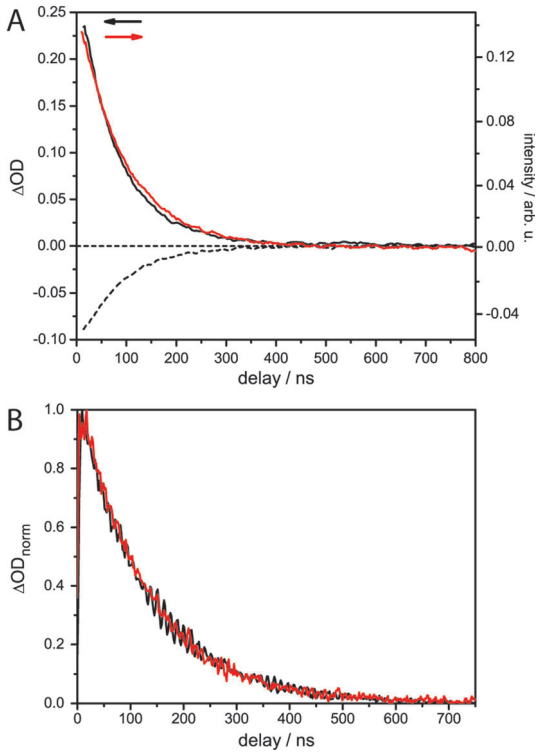


Fig. 3 (A) Transient absorption kinetics of **RuOs** at selected probe wavelengths: 450 nm (dash/black), 590 nm (solid/black) and emission decay at 750 nm (red solid). (B) Direct comparison of the decay kinetics at 600 nm probe wavelength for **Ru** (black) and **RuFeRu** (red).

For **Ru** and **RuFeRu**, although no Ru(II) $^3$MLCT emission is detectable at room temperature, transient absorption spectroscopy with ns time-resolution reveals the presence of a long-lived excited state. The excited state lifetimes of **Ru** and **RuFeRu** are 132 and 129 ns, respectively (Fig. 3), which is in good agreement with the lifetime determined for the analogues homo-bimetallic Ru(II) complex (145 ns).[66] The nearly identical values of their lifetimes and spectral shapes of the transient spectra of the long-lived excited state in **Ru** and **RuFeRu** (see ESI,† Fig. S8) point to a similar origin of the signals, *i.e.* an excited state connected with the Ru(II) center. Contributions of an Fe(II) excited state to the transient spectra are not expected on the timescale of the experiment, as Fe(II)-terpyridyl species show typically lifetimes $<$10 ns (see below).[17,29,36,76–78] The observation of an excited Ru(II) state suggests that energy transfer between the Ru(II) and the Fe(II) metal centers in **RuFeRu** occurs with much less than 100% efficiency.

### fs time-resolved spectroscopy

To identify and to follow possible energy transfer processes in the polynuclear systems **RuFeRu** and **RuOs** fs time-resolved TA spectroscopy was applied. To disentangle the contributions of the Ru(II) and Fe(II)/Os(II) centers to the observed photoinduced dynamics and to be able to identify possible interactions and transfer processes between the different metal centers, first the characteristic dynamics of each metal center is studied by selective excitation at carefully chosen excitation wavelengths.

In contrast to the Os(II) and the Fe(II) centers, selective excitation of the Ru(II) chromophore is not possible in the polymetallic species, hence the monometallic compound **Ru** serves as reference model for the Ru(II) intrinsic spectral signatures and dynamics.

Upon excitation at 520 nm, *i.e.*, in the Ru(II) $^1$MLCT band of **Ru**, the transient spectra (Fig. 4) are dominated by excited-state absorption (ESA) at probe wavelengths longer than 520 nm with a maximum at 630 nm. Below 500 nm negative signal contributions due to ground-state bleach (GSB) dominate. Within the first 100 ps the signal intensity increases and the minimum in the GSB at 482 nm vanishes, while the second minimum shifts from 432 to 418 nm. After 1000 ps the overall intensity starts to decay (by approximately 8% up to 8 ns).

The data was globally fitted with a sequential relaxation scheme. To describe the data four rates and an additional long-lived component, with a lifetime exceeding the observation window, had to be taken into account (Table 1). A feasible assignment of the processes and the species associated spectra (SAS) corresponding to the excited states contributing to the relaxation processes (Fig. 5) is displayed in Scheme 1. The sub-ps process can be related to internal vibrational energy redistribution (IVR) and intersystem crossing (ISC), which leads to the population of the manifold of vibrationally hot Ru(II) $^3$MLCT states within the first ~200 fs with a quantum yield close to unity.[53,79–83] The two components in the range of a few ps describe intramolecular relaxation processes: $\tau_2$ = 2 ps is assigned to vibrational cooling[23,53,71,82–86] and interligand electron transfer (ILET)[35] after which the lowest vibrationally relaxed Ru(II) $^3$MLCT state in the system is populated and $\tau_3$ = 15 ps describes further structural relaxation, *i.e.*, planarization of the bridging ligand, and as a consequence delocalization of the Ru(II) $^3$MLCT state beyond the terpyridine sphere of the bisterpyridine bridging ligand.[30,66] The slowest component $\tau_5$ responsible for the slight decay of the signal amplitude at later delay times can be identified as equilibration with a $^3$LC state (see ESI,† Fig. S10).[66] This equilibration is found to be approached much slower in the monometallic complex **Ru** than in the related homobimetallic complex **RuRu** (**Ru** $\tau_5$ = 3100 ps, **RuRu** $\tau$ = 361 ps[66]). This could be an indication for changes in the relative energetic positions of the $^3$MLCT and $^3$LC states induced by the coordination of the

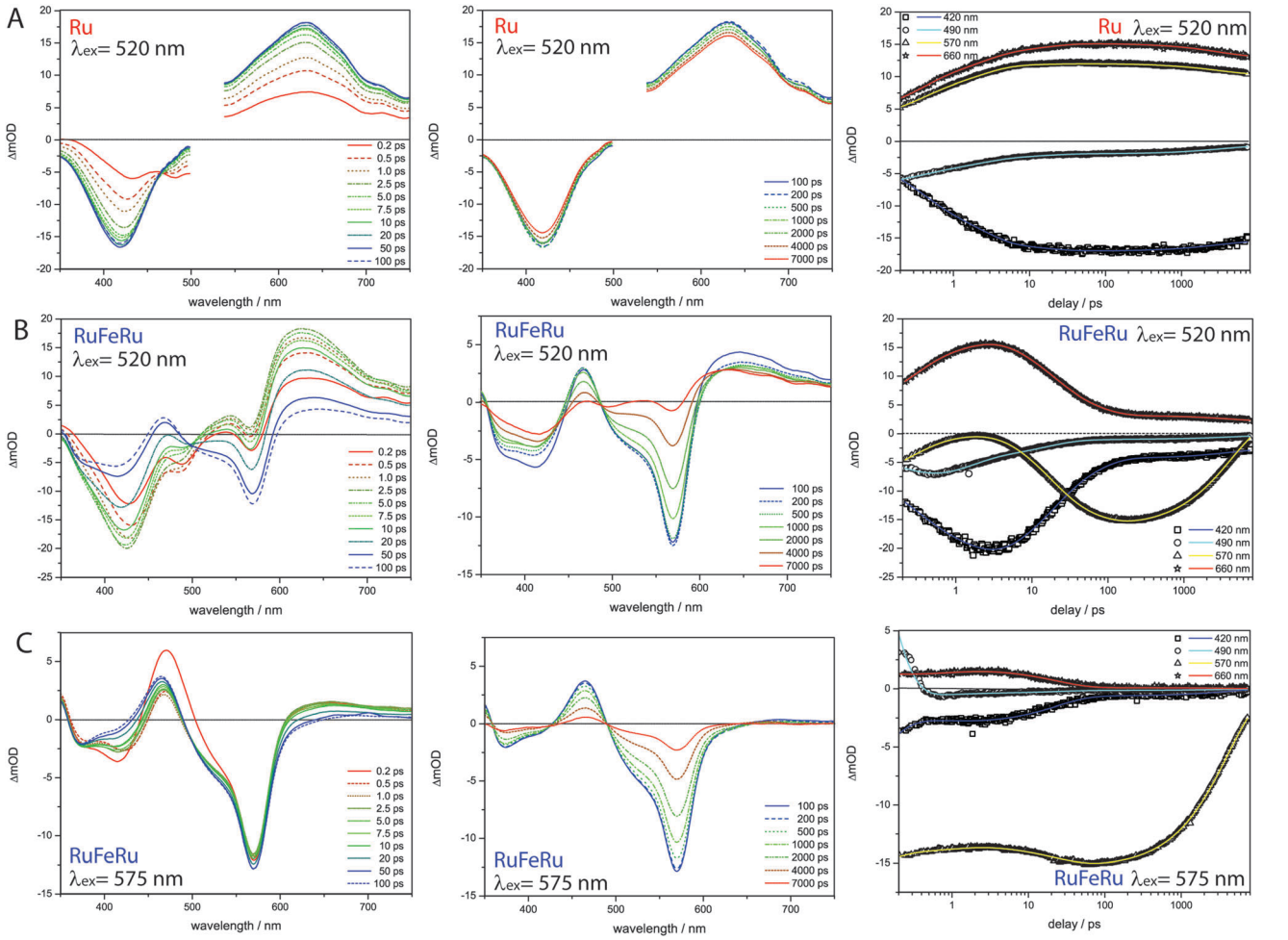


Fig. 4 Transient absorption spectra at selected delay times (left and middle) for (A) **Ru** following excitation at 520 nm, (B) **RuFeRu** upon excitation at 520 nm and (C) **RuFeRu** upon excitation at 575 nm in acetonitrile and the respective kinetics at selected probe wavelengths (right). The pump region for **Ru** is neglected in the data evaluation due to scattered pump.

 

Table 1 Fit results of fs and ns time-resolved transient absorption measurements in acetonitrile, $k$ represents rate constant for a certain process, $\tau$ is the corresponding reciprocal value given for convenience

| | $\lambda_{ex}$/nm | $k_1$/ps$^{-1}$ | $\tau_1$/ps | $k_2$/ps$^{-1}$ | $\tau_2$/ps | $k_3$/ps$^{-1}$ | $\tau_3$/ps | $k_4$/ps$^{-1}$ | $\tau_4$/ps | $k_5$/ps$^{-1}$ | $\tau_5$/ps | $k_6$/ns$^{-1}$ | $\tau_6$/ns | $k_{inf}$[a]/ns$^{-1}$ | $\tau_{inf}$[a]/ns |
|---|---|---|---|---|---|---|---|---|---|---|---|---|---|---|---|
| **Ru** | 520 | 3.1 | ≤0.3 | 0.48 | 2.0 | 0.066 | 15 | — | — | 0.00033 | 3100 | — | — | 0.0076 | 132 |
| **RuFeRu** model[b] | 520 | 4.1 | ≤0.2 | 0.74 | 1.4 | 0.067 | 15 | 0.018 | 56 | — | — | 0.24 | 4.2 | 0.0077 | 129 |
| **RuFeRu** | 575 | 9.7 | ≤0.1 | 0.92 | 1.1 | — | — | 0.043 | 23 | — | — | 0.25 | 4.1 | — | — |
| **RuOs** | 670 | — | — | 1.3 | 0.8 | 0.11 | 9 | — | — | 0.0016 | 650 | — | — | 0.01 | 100 |
| **RuOs** | 520 | 4.8 | ≤0.2 | 0.63 | 1.6 | 0.090 | 11 | — | — | 0.0014 | 700 | — | — | | |

[a] Infinite component in the fs time-resolved measurements, rate/lifetime determined by ns time-resolved TA and emission measurements. [b] Numerical fit applying model described in Scheme 1.

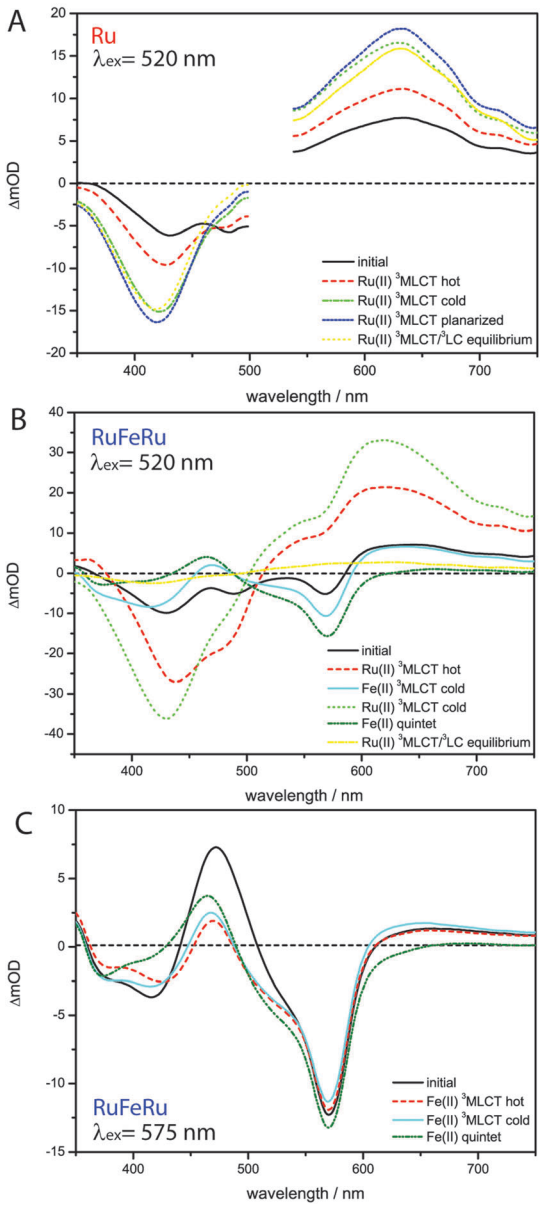


Fig. 5 SAS resulting from the global fit (A) **Ru** excitation 520 nm sequential model, (B) **RuFeRu** excitation 520 nm model with energy transfer according to Scheme 1, (C) **RuFeRu** excitation at 575 nm sequential model.

second metal center leading to changes in the activation barriers impacting the equilibration process.

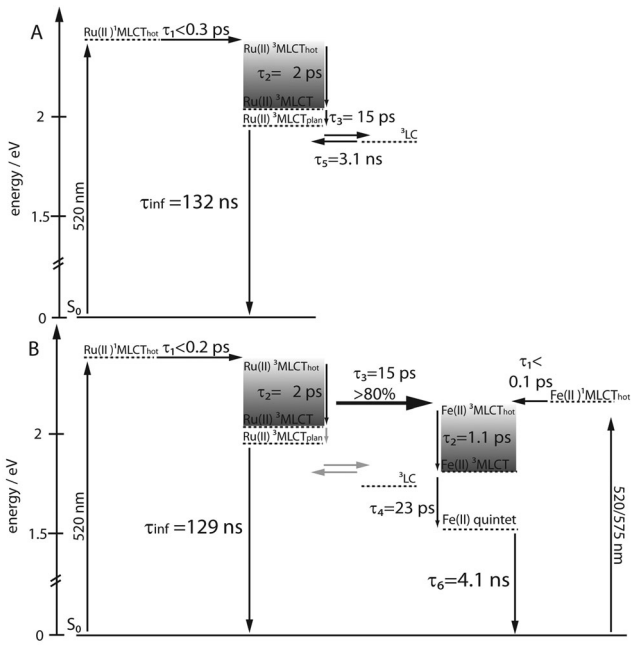


Scheme 1 Proposed relaxation schemes for **Ru** and **RuFeRu**, solid lines define energy levels with defined energetic positions, while dashed lines define excited states, the energy of which can only be indirectly inferred or depends on the excitation wavelength, processes in grey are not directly observable in the data.

Upon selective excitation of **RuFeRu** into the Fe(II) $^1$MLCT transition at 575 nm, the Fe(II) intrinsic dynamics is accessible (Fig. 4). Transient spectra show GSB at 570 nm corresponding to the maximum of the Fe(II) $^1$MLCT transition. Three regions dominated by ESA are observed: at wavelength longer than 605 nm, between 490 and 430 nm and in the UV below 360 nm. The ESA feature in the red spectral region decays within 100 ps. On the same timescale the second ESA feature gains intensity and broadens, extending further to the blue spectral range. After 100 ps a global decay of the overall signal intensity occurs. This development can quantitatively be described by a multi-exponential fit corresponding to the sequential relaxation scheme presented in Scheme 1 applying four exponentials (see Table 1 and Fig. 5 for SAS). The sub-ps and 1.1 ps processes describe – in analogy to the processes at the Ru(II) center – population of the Fe(II) $^3$MLCT manifold and vibrational cooling. Especially interesting is the process with a time constant of $\tau_4$ = 23 ps. This process is connected to the decay of the ESA feature in the red

probe range (see also decay associated spectra (DAS) in the ESI,† Fig. S10), which is – according to literature – a characteristic feature of the Fe(II) $^3$MLCT state.[37,38] Hence, the process associated with $\tau_4$ probably describes the depopulation of the Fe(II) $^3$MLCT state *via* $^3$MC states resulting in population of the high-spin Fe(II) quintet state. From the decay of the overall signal representing repopulation of the ground state a Fe(II) quintet lifetime of $\tau_6$ = 4.1 ns is determined, which is comparable to lifetimes reported for the quintet state of $[Fe(tpy)_2]^{2+}$.[17,29,36,76,77] Neither planarization nor formation of an equilibrium with an $^3$LC state is observed upon excitation of the Fe(II) center. The latter is probably due to the lower energetic position of the excited states of the Fe(II) center compared to the Ru(II) center, preventing a thermal population of the $^3$LC states, while the former might skip detection due to negligible spectral changes in the observation range. Nevertheless, from these results it can be concluded that the system at hand shows a lifetime of 23 ps for the Fe(II) $^3$MLCT state, which is the longest reported in literature.[50,51] Hence, the strong conjugated and extended ligand system shows a similar stabilizing effect on the Fe(II) $^3$MLCT state as for the Ru(II) $^3$MLCT states.

In the next step the photoinduced processes in **RuFeRu** upon excitation at 520 nm, where simultaneously excitation of Ru(II) $^1$MLCT and Fe(II) $^1$MLCT transitions occurs, are investigated. Immediately after excitation the transient spectra (Fig. 4) can be described as a superposition of the spectral characteristics of both centers at early delay times. During the first 100 ps the spectral features characteristic for the excited states of the Ru(II) center decay (*e.g.*, the strong ESA signal in the red probe range) while the characteristic signatures of the Fe(II) excited states (*e.g.*, bleach at 570 nm) gain in intensity. In the following the signal amplitude is decaying on a similar timescale as observed for the ground-state repopulation from the Fe(II) quintet state. Nonetheless, a residual amplitude remains beyond the time-scale of the experiment (8 ns). This long-lived species shows positive and negative signal above and below 500 nm, respectively, and thus reflects the transient spectra of the photoexcited Ru(II)-subunit at long delay times (see ESI,† Fig. S14). A simple multi-exponential fit assuming a superposition of the characteristic Ru(II) and Fe(II) centered photoinduced dynamics was not sufficient to describe the observed temporal development of the signal (see ESI,† Table S1 and Fig. S9). Hence, changes of the values of the rates of the processes at the Ru(II) center due to coordination of the second metal center and additional processes like energy transfer between the Ru(II) and the Fe(II) centers need to be taken into account. A further complication is that by applying a sum of exponential functions to model the data only a strictly parallel or sequential relaxation scheme can be analytically described.[87] Hence, to describe the data exactly a numerical fit based on the relaxation scheme in Scheme 1 was performed (Table 1): due to the very similar time constants and close resemblance of the spectral contributions of the sub-ps $\tau_1$ and cooling processes $\tau_2$ at both metal centers, the applied model regards the initial excited state as weighted mixture of Ru(II) and Fe(II) $^1$MLCT states. These states are decaying in parallel to the respective thermally relaxed $^3$MLCT states, described by a component $\tau_1 \leq 0.2$ ps representing population of the respective triplet manifolds. The component $\tau_2$ mainly represents the vibrational cooling at the Ru(II) center, contributions from cooling at the Fe(II) center are neglected, this process probably is not detectable due only minor changes in the SAS (Fig. 5) between Fe(II) $^3$MLCT$_{hot}$ and Fe(II) $^3$MLCT$_{cold}$. From the development of the spectral signature with time (Fig. 4), *i.e.* decay of the Ru(II) features and increase of the Fe(II) signatures on a timescale up to 50 ps, it can be deduced that the energy transfer from the Ru(II) center to the Fe(II) center occurs in parallel to or even before further relaxation (planarization and equilibration) at the Ru(II) center. The time constant for the energy transfer $\tau_3$ is found to be with 15 ps nearly identical to that describing the planarization in **Ru**. Further, a fraction of excitation remains at the Ru(II) center, which is indicated by the remaining residual Ru(II) signature beyond 8 ns. This suggests that in this system energy transfer might occur from a non-planarized state in parallel to planarization and a fraction of the excited molecules remains trapped in the energetically low-lying planarized Ru(II) excited state. From the intensity ratio of the long-lived component in the data of **Ru** and **RuFeRu** upon excitation at 520 nm the efficiency of the energy transfer from the Ru(II) center to the Fe(II) center is determined to be at least 80%, assuming that neither the extinction coefficient in the ground nor the excited state changes significantly upon coordination of the Fe(II) center (details see ESI†). In the model applied, equilibration at the Ru(II) center is not explicitly included. This process is expected to be slower than the energy transfer and occurs only in the residual fraction of the excited molecules remaining in the Ru(II) excited state, resulting in very weak contributions to the overall signal development, too low to be determined properly (see ESI,† Fig. S12). The final equilibrated Ru(II) state is considered in the fit by incorporation of a constant component. Hence, the further development of the signal represents Fe(II) centered kinetics only. The process associated with $\tau_4$ probably is connected to the depopulation of the $^3$MLCT state to form the Fe(II) quintet state. The reason for the observed deceleration of this process upon excitation at 520 nm compared to direct excitation at 575 nm remains unclear at the moment and is subject to further investigations. $\tau_6$ describes ground-state repopulation originating from the quintet state. The description of the experimental data applying this model results in SAS for the involved excited states, which are in good agreement with the spectra determined for the respective states at the Ru(II) and Fe(II) center from the reference measurements described above (Fig. 5). This resemblance confirms the validity of the applied model.

In contrast to **RuFeRu**, **RuOs** shows only minor differences in the dynamic behavior upon direct excitation of the $^3$MLCT of the Os(II) center at 670 nm and upon excitation at 520 nm, where $^1$MLCT transitions of both the Ru(II) and the Os(II) center are excited (Fig. 6). Under both conditions the transient spectra show strong GSB below 510 nm and a broad ESA feature at wavelengths longer than 510 nm. The ESA intensity increases during the first 10 ps, while the GSB intensity remains constant. After 10 ps the overall signal amplitude decays reaching a plateau at 80% of the maximum value of signal amplitude. Assuming excitation of both Ru(II) and Os(II) $^1$MLCT states at

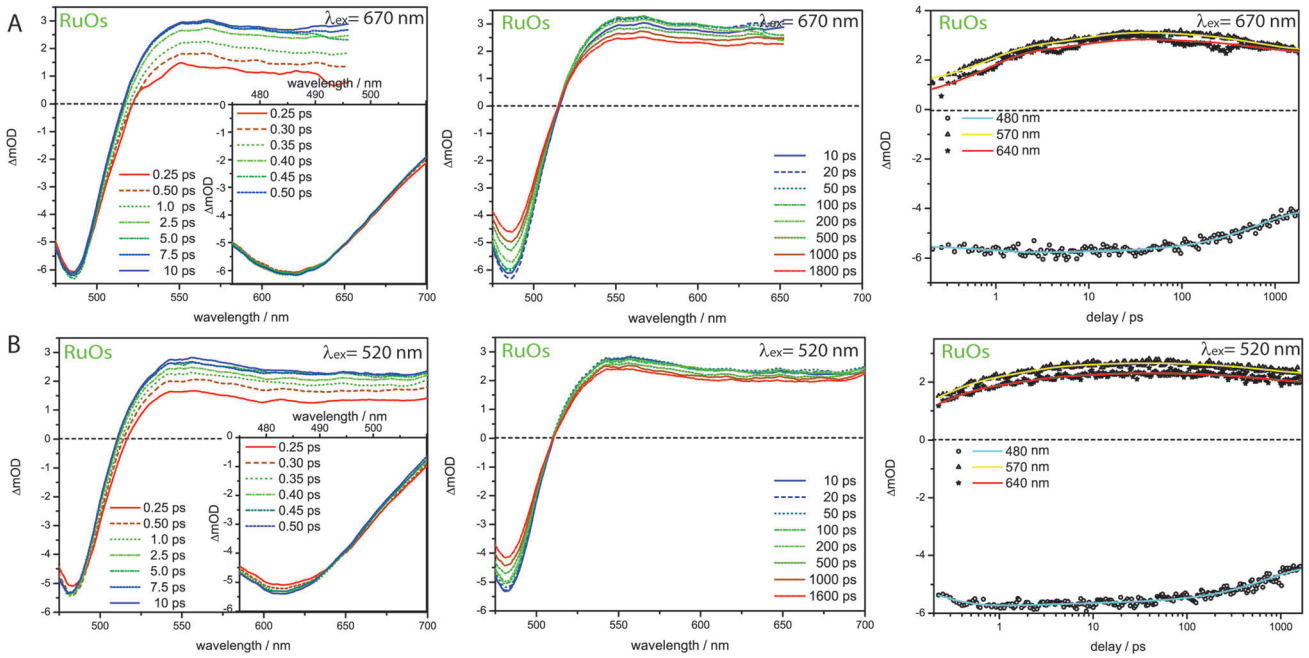


Fig. 6 Transient spectra and kinetic traces for **RuOs** upon excitation at (A) 670 nm and (B) 520 nm. The insets show a magnification of the ultrafast sub 0.5 ps development of the GSB region.

520 nm, the absence of signatures of Ru(II) excited states in the transient spectra suggests that the energy transfer from the Ru(II) to the Os(II) center occurs on an ultrafast timescale (<200 fs) with 100% efficiency and escapes detection due to the limited time-resolution of the experiment. Such highly efficient ultrafast energy transfer processes have been reported before for other multimetallic systems combining Ru(II) and Os(II) metal centers.[15,18,28,31,56,88–90] This assumption is corroborated by the results of the multi-exponential fit (Table 1): independent of the excitation conditions vibrational cooling (~1 ps), ligand planarization (~10 ps) and equilibration with the $^3$LC state (~600–700 ps) are observed. Further, the SAS (Fig. 7) for the involved excited states match each other very closely for varying excitation conditions and hence, the observed processes are assigned to occur in the Os(II) excited states manifold. The equilibration in **RuOs** between the Os(II) $^3$MLCT state and the $^3$LC state is slower than the equilibration between the Ru(II) $^3$MLCT states and the $^3$LC states in the homobimetallic complex **RuRu**,[66] which is probably due to different relative energetic positions between the respective $^3$MLCT state and the $^3$LC state and altered activation barriers, the Os(II) $^3$MLCT states are typically 0.20–0.3 eV lower in energy than the Ru(II) $^3$MLCT states.[17] The only difference in the pump-wavelength dependent data can be found on timescales <0.5 ps: here, an increase in GSB intensity and a slight blueshift in the maximum is present upon excitation at 520 nm (Fig. 6), which is described by the sub-ps component $\tau_1$ (Table 1). This component could be due to $^3$MLCT population processes from the excited $^1$MLCT states under these excitation conditions but could also show contributions of the energy transfer. However, to unambiguously assign these possible processes measurements with higher time resolution are necessary.

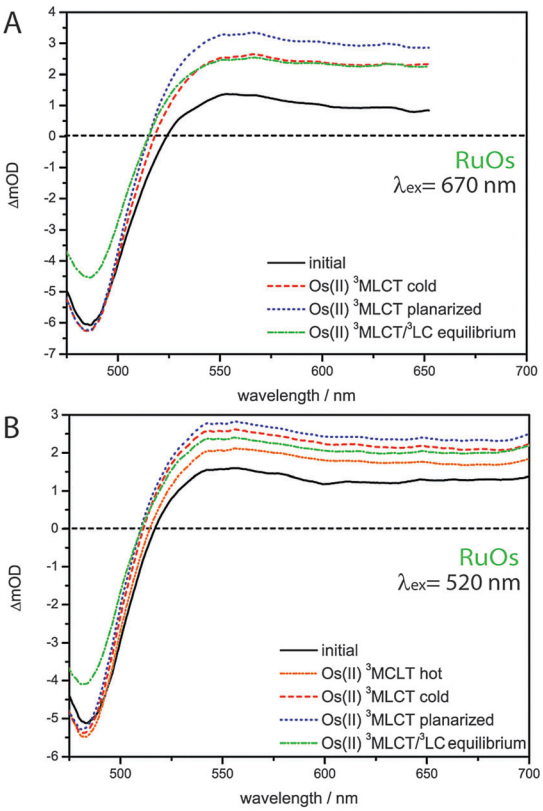


Fig. 7 SAS for **RuOs** resulting from a fit with a sequential model according to Scheme 2 upon excitation at (A) 670 nm and (B) 520 nm.

The effect that energy transfer occurs on the ultrafast time-scale and with 100% efficiency from Ru(II) to Os(II) centers while

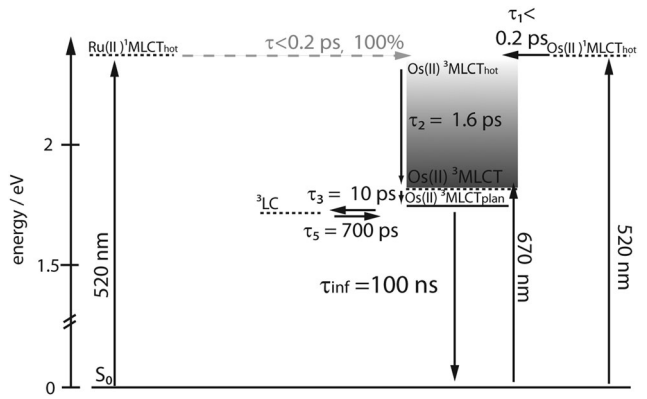


Scheme 2 Proposed relaxation scheme for **RuOs**, solid lines define energy levels with defined energetic positions, while dashed lines define excited states, the energy of which can only be indirectly inferred or depends on the excitation wavelength, processes in grey are not directly observable in the data.

in comparable systems combining Ru(II) and Fe(II) centers energy transfer to the lower lying Fe(II) centered states is slower and less efficient, has been observed before but no explanation was delivered.[56] In general, two mechanisms for energy transfer are distinguished: energy transfer *via* dipole–dipole interactions (Förster-type)[91] and energy transfer *via* electron-exchange mechanism (Dexter-type).[92] A precondition for the dipole mechanism to be efficient is that transitions with high oscillator strength at the donor and acceptor site are involved and spectral overlap between donor emission and acceptor absorption is necessary. Dexter transfer requires orbital overlap for efficient electron exchange and is usually discussed as short range mechanism, but the conjugated system of the ligand system can support long-range energy transfer of Dexter-type. The missing donor emission would rule out energy transfer by Förster-type in our systems, but the situation is more complicated, because the energy transfer originates from non-relaxed states. For the ultrafast energy transfer in **RuOs** two scenarios can be discussed:[15,88–90] singlet–singlet transfer and triplet–triplet transfer. For the triplet transfer mechanism, Dexter transfer might be favored, due to the low oscillator strength of the contributing triplet transitions though contributions of Förster transfer cannot be ruled out completely with the available data. For the transfer between the singlet states both Förster and Dexter mechanism could contribute, as the singlet states at both centers possess substantial oscillator strengths. Similar conclusions can be reached for the transfer mechanism in **RuFeRu**. As the oscillator strength of the radiative transitions from the non-relaxed $^3$MLCT state is not assessable from the available data, it is not possible to completely rule out a transfer following Förster mechanism, but a number of reports in literature suggest Dexter-type energy transfer between Ru(II) and Fe(II)-polypyridyl centers to be the most probable pathway.[93–97] Unfortunately, no further insight in the mechanism is possible with the available data, but the observed differences in the rates might be determined by which of the proposed routes is followed and simply be based on differences in the relative energy of donor and acceptor states.

## Summary and conclusion

In this investigation polymetallic complexes are investigated, which combine Ru(II) and Fe(II) (**RuFeRu**) or Os(II) (**RuOs**) bisterpyridine chromophores by coordination to an extended highly conjugated bis-4′-terpyridine bridging ligand. Due to their broad absorption range these mixed metal systems represent interesting candidates for light-harvesting antennae systems. Time-resolved spectroscopy reveals that energy transfer to the metal center with the lowest excited states in the assembly occurs in both systems with high efficiencies. While in **RuFeRu** an energy transfer of 80% occurs with a time constant of 15 ps from the Ru(II) to the Fe(II) center, the transfer from the Ru(II) to the Os(II) center in **RuOs** occurs on the ultrafast timescale $\leq$200 fs with unity quantum yield. These high efficiencies make these structures feasible candidates for incorporation into larger assemblies for long-range energy transfer.

The high conjugation of the bis-4′-terpyridyl ligand leads to a stabilization of the $^3$MLCT states resulting in a prolonged lifetime. This is of special importance with respect to the lifetime of the $^3$MLCT state at the Fe(II) center, which up to now limits the applicability of Fe(II) polypyridyl systems for collection of solar energy. The results presented in this study indicate that in these Fe(II)-terpyridyl structures with extended conjugated ligands an exceptional high $^3$MLCT lifetime of 23 ps is achieved, which is the longest reported in literature.

In summary, the investigations presented in this work demonstrate that the compounds employed may be suitable building blocks for light-harvesting antennas. Future work will focus on the transfer of these structural motives into oligomeric structures.

## Acknowledgements

We acknowledge support from Deutsche Forschungsgemeinschaft (DFG, Grant No. SCHU1229-16/1 and DI1517-3/1), LaserLab Europe (LLC001917), the Fonds der Chemischen Industrie and COST Action CM1202 Perspect-$H_2O$. The group at Würzburg acknowledges support by the SolTech Initiative of the Bavarian State Ministry of Science, Research and the Arts.

## References

1 T. Zhang and W. B. Lin, *Chem. Soc. Rev.*, 2014, **43**, 5982–5993.
2 P. D. Frischmann, K. Mahata and F. Würthner, *Chem. Soc. Rev.*, 2013, **42**, 1847–1870.
3 B. Albinsson, J. K. Hannestad and K. Borjesson, *Coord. Chem. Rev.*, 2012, **256**, 2399–2413.
4 J. Yang, M. C. Yoon, H. Yoo, P. Kim and D. Kim, *Chem. Soc. Rev.*, 2012, **41**, 4808–4826.
5 F. Puntoriero, A. Sartorel, M. Orlandi, G. La Ganga, S. Serroni, M. Bonchio, F. Scandola and S. Campagna, *Coord. Chem. Rev.*, 2011, **255**, 2594–2601.
6 M. Kozaki and K. Okada, *J. Synth. Org. Chem., Jpn.*, 2011, **69**, 1145–1157.
7 D. Gust, T. A. Moore and A. L. Moore, *Acc. Chem. Res.*, 2009, **42**, 1890–1898.

8 M. R. Wasielewski, *Acc. Chem. Res.*, 2009, **42**, 1910–1921.
9 F. Puntoriero, F. Nastasi, M. Cavazzini, S. Quici and S. Campagna, *Coord. Chem. Rev.*, 2007, **251**, 536–545.
10 F. Puntoriero, S. Serroni, M. Galletta, A. Juris, A. Licciardello, C. Chiorboli, S. Carnpagna and F. Scandola, *ChemPhysChem*, 2005, **6**, 129–138.
11 G. Calzaferri and K. Lutkouskaya, *Photochem. Photobiol. Sci.*, 2008, **7**, 879–910.
12 F. Odobel and H. Zabri, *Inorg. Chem.*, 2005, **44**, 5600–5611.
13 V. Balzani, A. Juris, M. Venturi, S. Campagna and S. Serroni, *Chem. Rev.*, 1996, **96**, 759–833.
14 C. Chiorboli, C. A. Bignozzi, F. Scandola, E. Ishow, A. Gourdon and J. P. Launay, *Inorg. Chem.*, 1999, **38**, 2402–2410.
15 J. Larsen, F. Puntoriero, T. Pascher, N. McClenaghan, S. Campagna, E. Åkesson and V. Sundström, *ChemPhysChem*, 2007, **8**, 2643–2651.
16 V. Balzani, G. Bergamini, F. Marchioni and P. Ceroni, *Coord. Chem. Rev.*, 2006, **250**, 1254–1266.
17 J. P. Sauvage, J. P. Collin, J. C. Chambron, S. Guillerez, C. Coudret, V. Balzani, F. Barigelletti, L. Decola and L. Flamigni, *Chem. Rev.*, 1994, **94**, 993–1019.
18 S. Welter, N. Salluce, P. Belser, M. Groeneveld and L. De Cola, *Coord. Chem. Rev.*, 2005, **249**, 1360–1371.
19 S. Welter, N. Salluce, A. Benetti, N. Rot, P. Belser, P. Sonar, A. C. Grimsdale, K. Mullen, M. Lutz, A. L. Spek and L. De Cola, *Inorg. Chem.*, 2005, **44**, 4706–4718.
20 A. Wild, A. Winter, F. Schlütter and U. S. Schubert, *Chem. Soc. Rev.*, 2011, **40**, 1459–1511.
21 A. Juris, V. Balzani, F. Barigelletti, S. Campagna, P. Belser and A. Vonzelewsky, *Coord. Chem. Rev.*, 1988, **84**, 85–277.
22 V. Balzani, G. Bergamini, S. Campagna and F. Puntoriero, *Photochemistry and Photophysics of Coordination Compounds I*, 2007, vol. 280, pp. 1–36.
23 A. Vlcek, *Coord. Chem. Rev.*, 2000, **200**, 933–977.
24 D. A. M. Egbe, B. Carbonnier, E. Birckner and U. W. Grummt, *Prog. Polym. Sci.*, 2009, **34**, 1023–1067.
25 A. C. Grimsdale, K. L. Chan, R. E. Martin, P. G. Jokisz and A. B. Holmes, *Chem. Rev.*, 2009, **109**, 897–1091.
26 R. Siebert, Y. X. Tian, R. Camacho, A. Winter, A. Wild, A. Krieg, U. S. Schubert, J. Popp, I. G. Scheblykin and B. Dietzek, *J. Mater. Chem.*, 2012, **22**, 16041–16050.
27 E. A. Medlycott and G. S. Hanan, *Chem. Soc. Rev.*, 2005, **34**, 133–142.
28 X. Y. Wang, A. Del Guerzo, S. Baitalik, G. Simon, G. B. Shaw, L. X. Chen and R. Schmehl, *Photosynth. Res.*, 2006, **87**, 83–103.
29 H. Cho, M. L. Strader, K. Hong, L. Jamula, E. M. Gullikson, T. K. Kim, F. M. F. de Groot, J. K. McCusker, R. W. Schoenlein and N. Huse, *Faraday Discuss.*, 2012, **157**, 463–474.
30 R. Siebert, A. Winter, U. S. Schubert, B. Dietzek and J. Popp, *Phys. Chem. Chem. Phys.*, 2011, **13**, 1606–1617.
31 C. Chiorboli, M. T. Indelli, F. Scandola, *Molecular Wires: From Design to Properties*, 2005, vol. 257, pp. 63–102.
32 C. Chiorboli, M. A. J. Rodgers and F. Scandola, *J. Am. Chem. Soc.*, 2003, **125**, 483–491.
33 L. Y. Zhu, A. Widom and P. M. Champion, *J. Chem. Phys.*, 1997, **107**, 2859–2871.
34 P. S. Wagenknecht and P. C. Ford, *Coord. Chem. Rev.*, 2011, **255**, 591–616.
35 J. T. Hewitt, P. J. Vallett and N. H. Damrauer, *J. Phys. Chem. A*, 2012, **116**, 11536–11547.
36 C. Creutz, M. Chou, T. L. Netzel, M. Okumura and N. Sutin, *J. Am. Chem. Soc.*, 1980, **102**, 1309–1319.
37 J. E. Monat and J. K. McCusker, *J. Am. Chem. Soc.*, 2000, **122**, 4092–4097.
38 W. Gawelda, A. Cannizzo, V. T. Pham, F. van Mourik, C. Bressler and M. Chergui, *J. Am. Chem. Soc.*, 2007, **129**, 8199–8206.
39 A. L. Smeigh, M. Creelman, R. A. Mathies and J. K. McCusker, *J. Am. Chem. Soc.*, 2008, **130**, 14105–14107.
40 C. Bressler, C. Milne, V. T. Pham, A. ElNahhas, R. M. van der Veen, W. Gawelda, S. Johnson, P. Beaud, D. Grolimund, M. Kaiser, C. N. Borca, G. Ingold, R. Abela and M. Chergui, *Science*, 2009, **323**, 489–492.
41 W. K. Zhang, R. Alonso-Mori, U. Bergmann, C. Bressler, M. Chollet, A. Galler, W. Gawelda, R. G. Hadt, R. W. Hartsock, T. Kroll, K. S. Kjaer, K. Kubicek, H. T. Lemke, H. Y. W. Liang, D. A. Meyer, M. M. Nielsen, C. Purser, J. S. Robinson, E. I. Solomon, Z. Sun, D. Sokaras, T. B. van Driel, G. Vanko, T. C. Weng, D. L. Zhu and K. J. Gaffney, *Nature*, 2014, **509**, 345–348.
42 C. Sousa, C. de Graaf, A. Rudavskyi, R. Broer, J. Tatchen, M. Etinski and C. M. Marian, *Chem. – Eur. J.*, 2013, **19**, 17541–17551.
43 G. Auböck and M. Chergui, *Nat. Chem.*, 2015, **7**, 629–633.
44 S. Ferrere and B. A. Gregg, *J. Am. Chem. Soc.*, 1998, **120**, 843–844.
45 D. N. Bowman, J. H. Blew, T. Tsuchiya and E. Jakubikova, *Inorg. Chem.*, 2013, **52**, 8621–8628.
46 D. G. Brown, N. Sanguantrakun, B. Schulze, U. S. Schubert and C. P. Berlinguette, *J. Am. Chem. Soc.*, 2012, **134**, 12354–12357.
47 S. U. Son, K. H. Park, Y. S. Lee, B. Y. Kim, C. H. Choi, M. S. Lah, Y. H. Jang, D. J. Jang and Y. K. Chung, *Inorg. Chem.*, 2004, **43**, 6896–6898.
48 L. Mercs and M. Albrecht, *Chem. Soc. Rev.*, 2010, **39**, 1903–1912.
49 Y. Z. Liu, T. Harlang, S. E. Canton, P. Chabera, K. Suarez-Alcantara, A. Fleckhaus, D. A. Vithanage, E. Goransson, A. Corani, R. Lomoth, V. Sundström and K. Wärnmark, *Chem. Commun.*, 2013, **49**, 6412–6414.
50 L. A. Fredin, M. Papai, E. Rozsalyi, G. Vanko, K. Warnmark, V. Sundstrom and P. Persson, *J. Phys. Chem. Lett.*, 2014, **5**, 2066–2071.
51 Y. Liu, K. S. Kjær, L. A. Fredin, P. Chábera, T. Harlang, S. E. Canton, S. Lidin, J. Zhang, R. Lomoth, K.-E. Bergquist, P. Persson, K. Wärnmark and V. Sundström, *Chem. – Eur. J.*, 2015, **21**, 3628–3639.
52 P. P. Laine, S. Campagna and F. Loiseau, *Coord. Chem. Rev.*, 2008, **252**, 2552–2571.
53 X. Y. Wang, A. Del Guerzo and R. H. Schmehl, *J. Photochem. Photobiol., C*, 2004, **5**, 55–77.
54 S. Baitalik, X. Y. Wang and R. H. Schmehl, *J. Am. Chem. Soc.*, 2004, **126**, 16304–16305.
55 D. Maity, S. Mardanya, S. Karmakar and S. Baitalik, *Dalton Trans.*, 2015, **44**, 10048–10059.
56 D. Maity, C. Bhaumik, S. Mardanya, S. Karmakar and S. Baitalik, *Chem. – Eur. J.*, 2014, **20**, 13242–13252.

57 A. K. C. Mengel, C. Forster, A. Breivogel, K. Mack, J. R. Ochsmann, F. Laquai, V. Ksenofontov and K. Heinze, *Chem. – Eur. J.*, 2015, **21**, 704–714.
58 L. Hammarström and O. Johansson, *Coord. Chem. Rev.*, 2010, **254**, 2546–2559.
59 M. Abrahamsson, M. Jager, T. Osterman, L. Eriksson, P. Persson, H. C. Becker, O. Johansson and L. Hammarstrom, *J. Am. Chem. Soc.*, 2006, **128**, 12616–12617.
60 M. Abrahamsson, M. Jager, R. J. Kumar, T. Osterman, P. Persson, H. C. Becker, O. Johansson and L. Hammarstrom, *J. Am. Chem. Soc.*, 2008, **130**, 15533–15542.
61 R. J. Kumar, S. Karlsson, D. Streich, A. R. Jensen, M. Jager, H. C. Becker, J. Bergquist, O. Johansson and L. Hammarstrom, *Chem. – Eur. J.*, 2010, **16**, 2830–2842.
62 F. Schramm, V. Meded, H. Fliegl, K. Fink, O. Fuhr, Z. R. Qu, W. Klopper, S. Finn, T. E. Keyes and M. Ruben, *Inorg. Chem.*, 2009, **48**, 5677–5684.
63 A. Breivogel, C. Forster and K. Heinze, *Inorg. Chem.*, 2010, **49**, 7052–7056.
64 A. Breivogel, C. Kreitner and K. Heinze, *Eur. J. Inorg. Chem.*, 2014, 5468–5490.
65 A. Breivogel, M. Meister, C. Forster, F. Laquai and K. Heinze, *Chem. – Eur. J.*, 2013, **19**, 13745–13760.
66 R. Siebert, C. Hunger, J. Guthmuller, F. Schlütter, A. Winter, U. S. Schubert, L. Gonzalez, B. Dietzek and J. Popp, *J. Phys. Chem. C*, 2011, **115**, 12677–12688.
67 A. Winter, C. Friebe, M. D. Hager and U. S. Schubert, *Eur. J. Org. Chem.*, 2009, 801–809.
68 B. Schulze, D. Escudero, C. Friebe, R. Siebert, H. Görls, S. Sinn, M. Thomas, S. Mai, J. Popp, B. Dietzek, L. Gonzalez and U. S. Schubert, *Chem. – Eur. J.*, 2012, **18**, 4010–4025.
69 K. Barthelmes, J. Kübel, A. Winter, M. Wächtler, C. Friebe, B. Dietzek and U. S. Schubert, *Inorg. Chem.*, 2015, **54**, 3159–3171.
70 F. Barigelletti, L. Flamigni, V. Balzani, J. P. Collin, J. P. Sauvage, A. Sour, E. C. Constable and A. M. W. C. Thompson, *J. Am. Chem. Soc.*, 1994, **116**, 7692–7699.
71 S. Campagna, F. Puntoriero, F. Nastasi, G. Bergamini and V. Balzani, *Photochemisty and Photophysics of Coordination Compounds I: Ruthenium*, Springer, Berlin, 2007.
72 R. Siebert, F. Schlutter, A. Winter, M. Presselt, H. Gorls, U. S. Schubert, B. Dietzek and J. Popp, *Cent. Eur. J. Chem.*, 2011, **9**, 990–999.
73 M. Presselt, B. Dietzek, M. Schmitt, S. Rau, A. Winter, M. Jager, U. S. Schubert and J. Popp, *J. Phys. Chem. A*, 2010, **114**, 13163–13174.
74 M. Presselt, B. Dietzek, M. Schmitt, J. Popp, A. Winter, M. Chiper, C. Friebe and U. S. Schubert, *J. Phys. Chem. C*, 2008, **112**, 18651–18660.
75 R. Siebert, A. Winter, B. Dietzek, U. S. Schubert and J. Popp, *Macromol. Rapid Commun.*, 2010, **31**, 883–888.
76 J. K. Mccusker, K. N. Walda, R. C. Dunn, J. D. Simon, D. Magde and D. N. Hendrickson, *J. Am. Chem. Soc.*, 1993, **115**, 298–307.
77 A. Hauser, C. Enachescu, M. L. Daku, A. Vargas and N. Amstutz, *Coord. Chem. Rev.*, 2006, **250**, 1642–1652.
78 G. Vankó, A. Bordage, M. Pápai, K. Haldrup, P. Glatzel, A. M. March, G. Doumy, A. Britz, A. Galler, T. Assefa, D. Cabaret, A. Juhin, T. B. van Driel, K. S. Kjær, A. Dohn, K. B. Møller, H. T. Lemke, E. Gallo, M. Rovezzi, Z. Németh, E. Rozsályi, T. Rozgonyi, J. Uhlig, V. Sundström, M. M. Nielsen, L. Young, S. H. Southworth, C. Bressler and W. Gawelda, *J. Phys. Chem. C*, 2015, **119**, 5888–5902.
79 J. N. Demas and D. G. Taylor, *Inorg. Chem.*, 1979, **18**, 3177–3179.
80 J. N. Demas and G. A. Crosby, *J. Am. Chem. Soc.*, 1971, **93**, 2841–2847.
81 A. I. Baba, J. R. Shaw, J. A. Simon, R. P. Thummel and R. H. Schmehl, *Coord. Chem. Rev.*, 1998, **171**, 43–59.
82 N. H. Damrauer, G. Cerullo, A. Yeh, T. R. Boussie, C. V. Shank and J. K. McCusker, *Science*, 1997, **275**, 54–57.
83 J. K. McCusker, *Acc. Chem. Res.*, 2003, **36**, 876–887.
84 M. Chergui, *Dalton Trans.*, 2012, **41**, 13022–13029.
85 A. C. Bhasikuttan, M. Suzuki, S. Nakashima and T. Okada, *J. Am. Chem. Soc.*, 2002, **124**, 8398–8405.
86 W. R. Browne, W. Henry, C. G. Coates, C. Brady, K. L. Ronayne, P. Matousek, M. Towrie, S. W. Botchway, A. W. Parker, J. G. Vos and J. J. McGarvey, *J. Phys. Chem. A*, 2008, **112**, 4537–4544.
87 I. H. M. van Stokkum, D. S. Larsen and R. van Grondelle, *Biochim. Biophys. Acta*, 2004, **1658**, 262.
88 H. B. Baudin, J. Davidsson, S. Serroni, A. Juris, V. Balzani, S. Campagna and L. Hammarström, *J. Phys. Chem. A*, 2002, **106**, 4312–4319.
89 J. Andersson, F. Puntoriero, S. Serroni, A. Yartsev, T. Pascher, T. Polivka, S. Campagna and V. Sundstrom, *Faraday Discuss.*, 2004, **127**, 295–305.
90 J. Andersson, F. Puntoriero, S. Serroni, A. Yartsev, T. Pascher, T. Polivka, S. Campagna and V. Sundstrom, *Chem. Phys. Lett.*, 2004, **386**, 336–341.
91 T. Förster, *Discuss. Faraday Soc.*, 1959, 7–17.
92 D. L. Dexter, *J. Chem. Phys.*, 1953, **21**, 836–850.
93 J. Lombard, J. C. Lepretre, J. Chauvin, M. N. Collomb and A. Deronzier, *Dalton Trans.*, 2008, 658–666.
94 J. Lombard, S. Romain, S. Dumas, J. Chauvin, M. N. Collomb, D. Daveloose, A. Deronzier and J. C. Lepretre, *Eur. J. Inorg. Chem.*, 2005, 3320–3330.
95 R. H. Schmehl, R. A. Auerbach, W. F. Wacholtz, C. M. Elliott, R. A. Freitag and J. W. Merkert, *Inorg. Chem.*, 1986, **25**, 2440–2445.
96 S. L. Larson, S. M. Hendrickson, S. Ferrere, D. L. Derr and C. M. Elliott, *J. Am. Chem. Soc.*, 1995, **117**, 5881–5882.
97 F. Lafolet, J. Chauvin, M. Collomb, A. Deronzier, H. Laguitton-Pasquier, J. C. Lepretre, J. C. Vial and B. Brasme, *Phys. Chem. Chem. Phys.*, 2003, **5**, 2520–2527.

 